Sowers, L. C., Fazakerley, G. V., Eritja, R., Kaplan, B. E., & Goodman, M. F. (1986a) *Proc. Natl. Acad. Sci. U.S.A.* (in press).
Sowers, L. C., Fazakerley, G. V., Kawaja, T. A., & Goodman, M. F. (1986b) (submitted for publication).
Sun, L., & Singer, B. (1974) *Biochemistry 13*, 1905–1913.
Topal, M. D., & Fresco, J. R. (1976) *Nature (London) 263*, 289–293.
Topal, M. D., & Warshaw, M. M. (1976) *Biopolymers 15*, 1755–1773.
Watson, J. D., & Crick, F. H. C. (1953) *Nature (London) 171*, 964–967.

Articles

Bending and Flexibility of Kinetoplast DNA†

Stephen D. Levene,‡ Hen-Ming Wu, and Donald M. Crothers*
Department of Chemistry, Yale University, New Haven, Connecticut 06511
Received October 7, 1985; Revised Manuscript Received March 3, 1986

ABSTRACT: We have evaluated the extent of bending at an anomalous locus in DNA restriction fragments from the kinetoplast body of *Leishmania tarentolae* using transient electric dichroism to measure the rate of rotational diffusion of DNA fragments in solution. We compare the rate of rotational diffusion of two fragments identical in sequence except for circular permutation, which places the bend near the center in one case and near one end of the molecule in the other. Hydrodynamic theory was used to conclude that the observed 20% difference in rotational relaxation times is a consequence of an overall average bending angle of 84 ± 6° between the end segments of the fragment that contains the bending locus near its center. If it is assumed that bending results from structural dislocations at the junctions between oligo(dA)·oligo(dT) tracts and adjacent segments of B DNA, a bend angle of 9 ± 0.5° at each junction is required to explain the observations. The extent of bending is little affected by ionic conditions and is weakly dependent on temperature. Comparison of one of the anomalous fragments with an electrophoretically normal control fragment leads to the conclusion that they differ measurably in apparent stiffness, consistent with a significantly increased persistence length or contour length in the kinetoplast fragments.

It is now generally agreed that DNA molecules can exist in a stably bent conformation, whose character is dictated by special features of base sequence (Marini et al., 1982; Levene & Crothers, 1983; Wu & Crothers, 1984; Hagerman, 1984). This conclusion, stated originally by Marini et al. (1982), is based on the anomalous gel electrophoretic properties of DNA restriction fragments isolated from the kinetoplast body of parasites (Kidane et al., 1984) and the unexpectedly rapid rotational diffusion of these fragments, implying a more compact conformation in solution. Wu and Crothers (1984) used gel electrophoresis to map the bending locus in a fragment isolated from *Leishmania tarentolae* to the sequence -CA_{5-6}T-, repeated at 10 base pair intervals. Because the repeated unit is in phase with the DNA helix screw, the small bends associated with the individual sequence elements add coherently. Levene and Crothers (1983) showed with an appropriate model for sequence-directed bending that computer modeling and molecular graphics predict the position of the bending locus in agreement with the gel electrophoresis experiments.

Our objective in this work is to analyze quantitatively the extent of bending in a DNA restriction fragment containing the *L. tarentolae* kinetoplast (K DNA) bending locus, using rotational dynamics in an experimental approach analogous to that reported by Hagerman (1984). However, we sought to avoid the dubious assumption that the stiffness and contour length of K DNA, as measured by the persistence length P and the rise per base pair h, respectively, are the same as for a DNA fragment of unrelated sequence. Hence, we adopt the strategy used by Wu and Crothers (1984) in mapping the bending locus by gel electrophoresis, namely, to compare the properties of molecules that are identical in sequence except for circular permutation, thus placing the bend either at the middle or near the end of the molecule. As a consequence, comparative measurements refer to molecules of closely related sequence, which are nevertheless quite different in overall shape. While this approach does not eliminate possible problems resulting from variations of P with sequence along a given molecule, it does reduce the error from that source. Primarily because of this difference in experimental approach, our results show that the angular deformation of the helix axis at a bending locus is 2–3 times larger than the bending reported by Hagerman (1984).

Structural interpretation of the observed molecular dimensions from rotational dynamics requires a specific model, of which several have been proposed to account for the sequence-directed bending of DNA in solution. These include deformational anisotropy or wedge bending at ApA dinucleotides (Trifonov & Sussman, 1981; Marini et al., 1982; Levene & Crothers, 1983; Prunell et al., 1984), bending at junctions between regions of different helical structure (Selsing et al., 1979; Levene & Crothers, 1983; Wu & Crothers, 1984), and purine clash (Hagerman, 1984; Zhurkin, 1985), on the basis of Calladine's analysis of DNA structure (Calladine,

†Supported by Grant GM 21966 from the National Institutes of Health.
‡Present address: Department of Chemistry, University of California, San Diego, La Jolla, CA 92093.

0006-2960/86/0425-3988$01.50/0

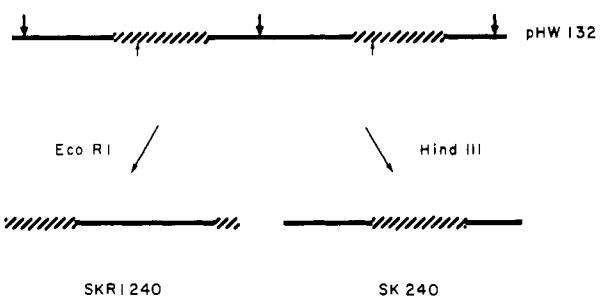

FIGURE 1: Methodology for preparing circularly permuted fragments. Plasmid pHW 132 consists of tandemly repeated multiple copies of SK 240 cloned into the *Hin*dIII site of plasmid pJW 37 (Wu & Crothers, 1984). Restriction sites for *Hin*dIII and *Eco*RI are designated by the heavy and light arrows, respectively; the hashed area is the 100 bp of DNA whose center coincides with the center of bending as determined by Wu and Crothers (1984).

1982). We have chosen to interpret our data using the junction-bending model, although the principal results such as the overall angle at the bending locus and the apparent persistence length are little affected by this choice.

The junction-bending model was selected because, first, it appears to explain readily the data from other studies, which show that bending in kinetoplast DNA can be reversed by low levels of distamycin binding (Wu & Crothers, 1984). Second, application of the ApA wedge model, where non-zero tilt or roll is ascribed to ApA dinucleotides, sometimes predicts properties of unrelated sequences inconsistent with experimental observations; fragments that are predicted to be significantly bent are found to have essentially normal gel mobilities (unpublished results). Third, the junction-bending model easily explains the ability of elevated temperature to cause the mobility of K DNA fragments to revert to nearly normal values (Wu, 1982; Marini et al., 1984), since one need only postulate a conformational equilibrium in the A_{5-6} runs; increased temperature favors the B form and reduces the bending by removing the junctions with adjacent segments of B DNA.

The two restriction fragments of circularly permuted sequence used in this study were prepared from tandem repeats of a single fragment, in this case a 240-bp *Hin*dIII fragment containing a single bending locus (Wu & Crothers, 1984), as shown in Figure 1. The anomalies in the gel electrophoretic mobilities are of strikingly different degree for the *Hin*dIII and *Eco*RI fragments, hereafter referred to as SK 240 and SKRI 240, respectively; the ratio of apparent size to known size in a 5% polyacrylamide gel is 1.9 for SK 240 and 1.2 for SKRI 240.

The ratio of rotational relaxation times for these two fragments $R = \tau_{SK}/\tau_{SKRI}$ is interpreted by employing hydrodynamic models for systematically bent DNA chains. By use of a Monte Carlo method, rotational relaxation times are calculated for ensembles of model chains containing sequence-dependent bend angles and obeying wormlike chain statistics, thereby allowing for thermal flexibility as well as systematic bending. Zimm (1980) reported the first application of Monte Carlo methods for calculating the hydrodynamic properties of polymer chains and showed that the numerical method gives superior results to classical techniques based on the Kirkwood–Riseman preaveraging approximation (Kirkwood & Riseman, 1948). Application of the Monte Carlo method to the rotational dynamics of wormlike chains was made by Hagerman and Zimm (1981); we use an extension of their algorithm in our analysis.

Once the junction bend angle is known, the apparent persistence length P_{app} can be determined for the fragments used in this study. We show that P_{app} is consistently larger for the kinetoplast fragments than for an unrelated control fragment having normal gel electrophoretic mobility. Although P_{app} is not a direct measure of flexibility because of possible variations in the rise per base pair among different fragments, the result is significant because it suggests that measurable sequence-dependent variations in persistence length and unit rise can occur among DNA molecules.

Materials and Methods

Restriction Fragment Preparation. Plasmid pHW 132 was prepared by the alkaline lysis procedure of Maniatis et al. (1982). The DNA fragments SK 240 and SKRI 240 were prepared by digesting the plasmid overnight with *Hin*dIII or *Eco*RI at 37 °C in the appropriate restriction enzyme buffer at enzyme concentrations ranging from 0.2 to 1 unit/μg of DNA. A 267 base pair (bp) restriction fragment identical in size and sequence with a *Hae*III digestion product of pBR 322 was prepared by incubating pHW 132 under the above conditions in the presence of equal amounts of *Hin*dIII and *Hae*III. Reactions were stopped by extracting once with phenol and once with chloroform–isoamyl alcohol (24:1), followed by alcohol precipitation. The mixture of fragments, redissolved in TE buffer [10 mM tris(hydroxymethyl)-aminomethane hydrochloride (Tris-HCl), 1 mM disodium ethylenediaminetetraacetate (Na_2EDTA), pH 8.0] was layered onto a preparative 5 or 8% polyacrylamide slab gel (30 cm × 10 cm × 0.3 cm), which had been preelectrophoresed in TBE buffer (50 mM Tris–borate, 1 mM Na_2EDTA, pH 8.3). Bands containing the fragments were first located by briefly illuminating the gel with short-wavelength UV light against a fluorescent background and then excised with a scalpel. DNA fragments were recovered from the gel slices by electrophoretic elution in half-strength TBE buffer and applied to small DE-52 ion-exchange columns, washed with several hundred column volumes of 10 mM Tris-HCl and 0.1 M NaCl, pH 8.0, and eluted with approximately 1 column volume of TE buffer containing 1 M NaCl. Fragments were stored at −20 °C in TE buffer. All samples ran as single bands on 5 and 8% polyacrylamide gels.

Preparation of the DNA fragments for transient electric dichroism measurements involved a series of dialysis steps to remove trace amounts of multivalent ions and other contaminants. Fragments were first precipitated from 2 M ammonium acetate and 50% 2-propanol, redissolved, and dialyzed against 10 mM Tris-HCl, 25 mM Na_2EDTA, and 0.1 M NaCl, pH 8.0. Excess EDTA was removed by dialyzing the DNA solution extensively against TE buffer containing 0.1 M NaCl. The final preparative step consisted of extensive dialysis against the buffer used in the dichroism measurements.

Transient Electric Dichroism Measurements. The apparatus used in these studies is the same as described earlier (Marini et al., 1982), with one significant modification: two Cober 605-P pulse generators were used in series to provide voltages of up to 4 kV or electric field pulses of up to 8 kV/cm across the 0.5-cm electrode gap in the dichroism cell. Rotational relaxation times were determined by interactively fitting the decay portion of the dichroism signals to a linear combination of exponentials with standard nonlinear least-squares methods (Marquardt, 1963). Values of the rotational relaxation time were independent of the field strength for fields from 2.0 to 8.0 kV/cm, independent of the pulse width for pulses from 8 to 30 μs long and independent of DNA concentration over the range 15–40 μM base pairs. The cell temperature was maintained to within ±0.1 °C of the stated value and remained constant over the course of an experiment.

Theoretical Methods. Monte Carlo calculations of the rotational relaxation times were based on the algorithm of Hagerman & Zimm (1981); the differences in approach are detailed here:

(i) DNA chains consisting of N base pairs were modeled as an array of $N-1$ vectors with $3N-3$ coordinates specifying the configuration of the chain. The orientation of the ith vector in the $i-1$ coordinate frame is given by the ordered triple (θ_i, ϕ_i, ψ_i) as described previously by Levene and Crothers (1983), where the tilt angles θ_i and the roll angles ϕ_i are angular displacements in the x–z and y–z planes, respectively, and ψ_i are the twist angles about the helix axis. This parameterization of the chain configuration was used to maintain phasing between sequence elements while enabling the force constants for bending of the chain to be related to those for the wormlike chain. The probability distribution function for θ_i and ϕ_i is given by

$$p(\theta_i,\phi_i)\, d\theta_i\, d\phi_i = C \exp\left[-\frac{(\theta_i - \theta_i^0)^2}{2a^2} - \frac{(\phi_i - \phi_i^0)^2}{2b^2} \right] d\theta_i\, d\phi_i \quad (1)$$

with C a normalization constant and a and b chosen according to

$$a^2 + b^2 = 2h/P \quad (2)$$

where h is the unit rise of the helix and P is the persistence length. The angles θ_i and ϕ_i are therefore independent, normally distributed random variables with the mean values θ_i^0 and ϕ_i^0 specified as a function of DNA sequence according to the structural model considered. The methods used for obtaining normally distributed random numbers have been described elsewhere (Levene & Crothers, 1986). Nonfluctuating values for the torsion angles ψ_i^0 were determined by the particular model chosen.

(ii) The number of Stokes spheres m used to represent an individual chain was specified at the beginning of each calculation. The radius of the spheres σ was fixed by the condition that the volume of the model chains be equal to that of a rigid cylinder of radius $\rho = 13$ Å and length $(N-1)h$. Hence

$$\sigma = [3(N-1)\rho^2 h/(4m)]^{1/3} \quad (3)$$

The coordinates of the spheres were determined by first locating the centers of the terminal spheres at the chain ends. The remaining spheres were then equally spaced along the contour. Absolute and relative values of the rotational relaxation times were quite insensitive to sphere radius and spacing as long as the terminal beads coincided with the ends of the chain, consistent with the observations of Hagerman and Zimm (1981). In no case was the linear density of beads high enough for adjacent beads to overlap.

(iii) The form of the Oseen tensor **T**, given by Hagerman and Zimm (1981), is incorrect as written. The correct form given by Yamakawa (1970) was used to compute the hydrodynamic interactions between pairs of spheres i and j:

$$\mathbf{T}_{i,j} = (8\pi\eta_0 r_{i,j})^{-1}\left[\left(\mathbf{I} + \frac{\vec{r}_{i,j}\vec{r}_{i,j}}{r_{i,j}^2} \right) + \frac{2\sigma^2}{r_{i,j}^2}\left(\frac{1}{3}\mathbf{I} - \frac{\vec{r}_{i,j}\vec{r}_{i,j}}{r_{i,j}^2} \right) \right] \quad (4)$$

where **I** is the unit tensor, $\vec{r}_{i,j}$ is the vector between the centers of the ith and jth beads, $r_{i,j}$ is the length of this vector, and η_0 is the viscosity of the solvent.

(iv) The formal solution of the hydrodynamic equations was used throughout. For each configuration, the matrix of coefficients in the system of linear equations was factored by the LINPAK routine for symmetric indefinite matrices SSIFA. This system was solved for three different choices of the axis of rotation, with the LINPAK routine SSISL to obtain the unknown $3m$ components of the forces on the spheres. The rotational diffusion tensor was evaluated and diagonalized, and its principal values were averaged over the ensemble. The transverse (longest) rotational relaxation time τ^{MC} was computed from the principal elements D_1, D_2, and D_3 according to Wegener et al. (1979):

$$1/\tau^{MC} = 6D - 2B \quad (5)$$

where

$$D = (1/3)(D_1 + D_2 + D_3) \quad (6a)$$

and

$$B = (D_1^2 + D_2^2 + D_3^2 - D_1D_2 - D_2D_3 - D_1D_3)^{1/2} \quad (6b)$$

Calculations were programmed in FORTRAN-77 and run on a VAX 11/750 computer. A single simulation run for an ensemble of 500 chains 240 base pairs in length, each chain modeled by 20 Stokes spheres, consumed approximately 15 min of central processor time.

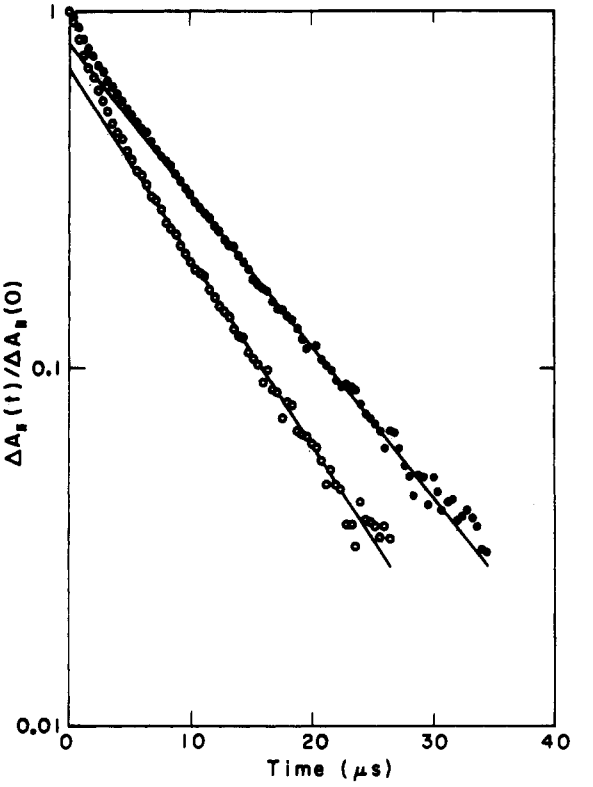

FIGURE 2: Semilogarithmic plot of the decay portion of the electric dichroism signal for SKRI 240 (●) and SK 240 (○) in 1.0 mM Tris-HCl and 0.025 mM $MgCl_2$, pH 8.0. Experimental conditions were $T = 6.0$ °C, field strength = 8.0 kV/cm, and pulse width = 12 μs. The solid lines give the best least-squares fits to the longest relaxation times; these were $\tau_{SK} = 8.2$ μs and $\tau_{SKRI} = 10.2$ μs.

RESULTS

The Kinetoplast Fragment Is Strongly Bent in Solution. Figure 2 shows data from transient electric dichroism measurements on samples of SK 240 and SKRI 240. The ratio R of measured rotational relaxation times can be used to determine the angular displacement of the helix axis at helix junctions if both molecules are assumed to have the same value for the persistence length P and if the resistance to thermal

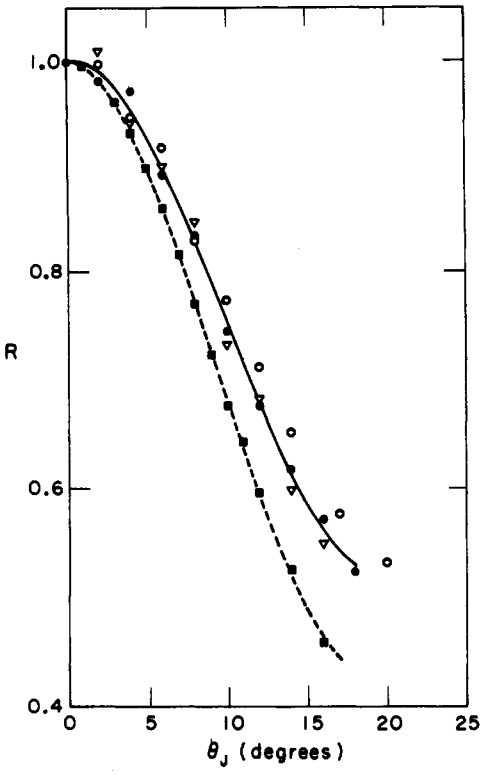

FIGURE 3: Ratios of rotational relaxation times, $R = \tau_{SK}/\tau_{SKRI}$, computed from Monte Carlo simulations of bent chains according to the junction-bending model. Configurational parameters for chains were computed according to the rule that $\theta_i^0 = \theta_J$ if a tract of five or more A's begins at residue $i + 1$, $\theta_i^0 = -\theta_J$ if a tract of five or more A's ends at residue i, and $\theta_i^0 = 0$ otherwise. ψ_i was set equal to 36.0° for tracts of five or more A's and equal to 34.3° otherwise; ϕ_i^0 was set equal to zero for all i. Data are shown for three different values of the parameters $a = b = (h/P)^{1/2}$, which correspond to values of P for an isotropic wormlike chain of P = 500 (○), 650 (●), and 800 Å (▽). The solid curve is the least-squares fit of a cubic equation to the data for P = 650 Å. The dashed curve is the least-squares fit of a cubic equation to data for rigid bent chains (■) with $\theta_i = \theta_i^0$ and $\phi_i = 0$ for all residues i. Ignoring residual flexibility has significant effects on the apparent value of θ_J. For example, a value of R = 0.8 corresponds to θ_J = 9.0° if P = 650 Å and θ_J = 7.4° if $P = \infty$; overall angular displacements of the ends of SK 240 in these two cases correspond to 84° and 66°, respectively. Neglecting residual flexibility therefore causes overall bending to be underestimated by approximately 20%. Results for finite values of P were obtained from pairs of independent simulations for ensembles of 500 chains modeled as 20 Stokes spheres. The estimated combined uncertainty in R for these results is approximately 3%.

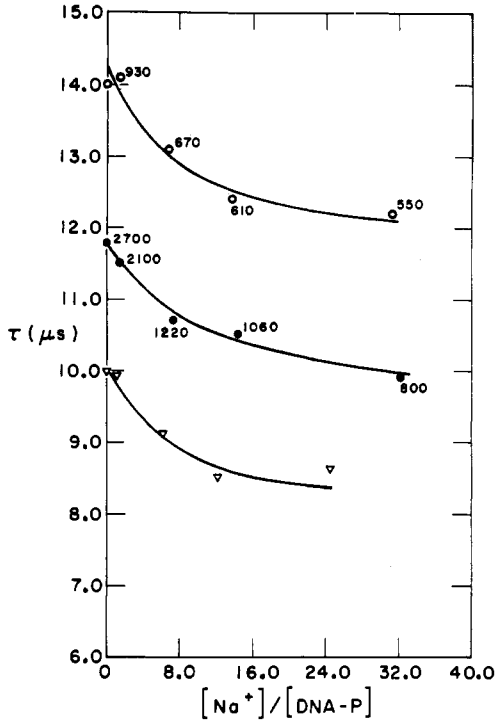

FIGURE 4: Dependence of rotational relaxation times τ on the ratio of added NaCl to DNA phosphate. Data points are 267-bp control (○), SKRI 240 (●), and SK 240 (▽). T = 6.0 °C. All samples initially contained 0.01 mM Na_2EDTA; samples for all measurements except the one at lowest NaCl concentration were prepared by mixing an aliquot of the DNA solution with stock solutions of NaCl. The numbers next to each data point correspond to the apparent persistence length (in Å) determined from a Monte Carlo analysis of the rotational relaxation time as described in the text. Simulations used an isotropic wormlike chain model for the 267-bp control and the junction-bending model with θ_J = 9.0° for SKRI 240. Ensembles of 700 chains were used in the determination of P; the estimated uncertainty in P, including the uncertainty in θ_J, is 10%.

bending in these fragments is assumed to be distributed uniformly along the contours of the two molecules. In Figure 3, we show that, within the limits set by the stated assumptions, the junction bend angle θ_J may be determined quite accurately from R even if the exact value of P is not known. Values of R computed by the Monte Carlo method for the same values of θ_J vary by less than 5% over a 2-fold change in P. This range of R values is not much larger than the statistical uncertainty in the Monte Carlo calculations; θ_J can therefore be determined by interpolation with the best fit curve to the Monte Carlo data for a single value of P. The value of θ_J corresponding to R = 0.80 is 9.0 ± 0.5°, leading to an angular displacement of 84 ± 6° between the two ends of SK 240. This value applies to the conditions cited in Figure 2, 1.0 mM Tris-HCl and 25 μM $MgCl_2$, but as shown in subsequent figures, the ratio R and, hence, the calculated bending angle are not strongly dependent on ionic conditions.

One referee pointed out that the τ values given in the caption to Figure 2 are larger than expected from our earlier measurements on a larger fragment of kinetoplast DNA (Marini et al., 1982). This is due to the fact that the τ values reported in the earlier study were obtained from single-exponential fits to the dichroism decay curves, which contain at least two exponential components. The τ values reported here correspond to the terminal component of a multiple exponential fit to the dichroism decay curves.

Kinetoplast Fragments Display Increased Apparent Stiffness Relative to a Normal Fragment. Use of the Monte Carlo approach to interpret the rotational diffusion of systematically bent DNA fragments permits P_{app} to be estimated from τ if the unit rise h is known. P_{app} values determined from experimental τ values for an electrophoretically normal 267-bp *Hae*III fragment and SKRI 240 are given in Figures 4 and 5 for a wide range of ionic conditions. The *Eco*RI fragment that contains the bending locus at one end was chosen for these detailed studies to minimize possible errors in P_{app} resulting from experimental uncertainty in the value of θ_J and from possible changes in θ_J with ionic strength.

The τ values obtained directly from the Monte Carlo simulations are not exact due to the limitations of modeling a flexible cylinder by a relatively small number of beads. The deficiencies of the model can be corrected for by assuming that the deviation of the Monte Carlo value τ^{MC} from the true value for the flexible molecule of length L, τ, equals the deviation of the value for the rigid bead-cylinder model τ_{CYL}' from that for a true smooth circular cylinder of the same length, τ_{CYL} (volume-corrected, as described above). Corrected τ values

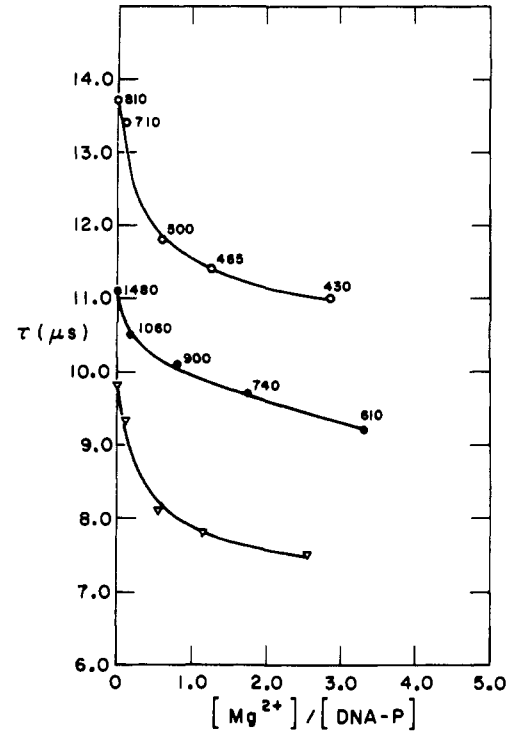

FIGURE 5: Rotational relaxation times at $T = 6.0$ °C as functions of the ratio of $MgCl_2$ added to the concentration of DNA phosphate. All samples contained 1.0 mM Tris-HCl, pH 8.0; Mg^{2+} concentrations were adjusted by adding an appropriate amount of $MgCl_2$ from stock solutions made up in the same Tris buffer. Symbols are the same as in Figure 4. Values for the apparent persistence length (in Å) determined from the Monte Carlo analysis described in the text are indicated next to each data point.

to be compared with experiment are then obtained from the expression

$$\tau = \tau^{MC}(\tau_{CYL}/\tau_{CYL}') \quad (7)$$

with τ_{CYL} computed from Broersma's (1960) expression:

$$\tau_{CYL} = \left(\frac{\eta_0 \pi L^3}{18 K_B T}\right)(\ln 2\alpha - \gamma)^{-1} \quad (8a)$$

where α is the ratio of chain length to diameter and γ is a correction for end effects given by

$$\gamma = 1.57 - 7\left(\frac{1}{\ln 2\alpha} - 0.28\right)^2 \quad (8b)$$

We assume that the same correction factor τ_{CYL}/τ_{CYL}' applies to both bent and linear molecules with the same values of L and m and is independent of θ_J. Further tests of this assumption depend on alternative methods for calculating the rotational relaxation time of smoothly bent rigid cylinders. The corrections are small, however, generally less than 1%.

Values of P_{app} for SKRI 240 were obtained from simulations with $\theta_J = 9.0°$, varying the value of P appearing in eq 2. P_{app} was determined from the experimental ratio τ_{SKRI}/τ_{CYL} by interpolation along a curve plotting $\tau^{MC}_{SKRI}/\tau_{CYL}'$ as a function of P (data not shown). P_{app} for the 267-bp DNA fragment was obtained from a cubic polynomial in L/P fitted to Monte Carlo data for unbent (linear) wormlike chains with systematically chosen values for L and P (data not shown). The choice of $\theta_J = 0°$ for the 267-bp fragment was based on convenience and on the fact that the DNA sequence contains only one oligo(dA)·oligo(dT) tract of more than three base pairs, located near one end of the molecule (Sutcliffe, 1977). Setting $\theta_J = 9.0°$ in a few simulations of the 267-bp control had no measurable effect on the computed τ value.

As shown in Figures 4 and 5, P_{app} for SKRI 240 is substantially higher than the value for the 267-bp control fragment over the entire range of added Na^+ and Mg^{2+} concentrations studied. The difference in P_{app} becomes more pronounced with decreasing salt concentration, indicating a significant electrostatic component. A change in the bend angle too small to result in a measurable change in R may contribute to this effect. However, even in the presence of 0.2 mM Mg^{2+}, where most of the electrostatic component of P is neutralized (Hagerman, 1983), P_{app}(SKRI) still exceeds P_{app}(267) by about 45%, as shown in Figure 5.

The foregoing analysis assumes that the average unit rise h is identical in both the 267-bp fragment and the kinetoplast fragment. Because τ depends strongly on L, a larger value of the average rise per base pair in SKRI 240 could account for the larger than expected value of τ_{SKRI} observed. Since only a few parameters can be determined experimentally in the present study, it is not possible to simultaneously extract h and P from data for a given fragment. The apparent unit rise for SKRI 240 can be determined, however, by assuming that h is known for the 267-bp control fragment and that the value of P estimated from τ_{267} is the same for both fragments. Preliminary simulations to evaluate τ_{SKRI}/τ_{267} as a function of the difference in unit rise have been carried out varying h_{SKRI} at constant values of P_{SKRI}. If it is assumed that $h_{267} = 3.40$ Å and $P_{SKRI} = P_{267} = 500$ Å, corresponding approximately to conditions described in the legend to Figure 2, the value of h_{SKRI} consistent with the experimental ratio τ_{SKRI}/τ_{267} is found to be equal to 3.50 Å, a difference of only 3%. The value of h_{SKRI} depends markedly on the estimated value of P and may also vary with ionic conditions, perhaps accounting partly for differences in the behavior of P_{app} with added salt concentration in the two fragments.

Extent of Bending Is Only Weakly Dependent on Ionic Strength. The flexibility of DNA at low ionic strengths, as with other linear polyelectrolytes, is dominated by electrostatic repulsion between like charges along the helix backbone. Electrostatic interactions may also significantly affect the observed extent of bending. Specific interactions of counterions with the altered helical form giving rise to the junction bends might stabilize the bent conformation. In addition, more effective screening of the intramolecular electrostatic interactions at higher ionic strength might be expected to increase the amount of bending in the fragment by lowering the overall charge density of the molecule and reducing repulsion between the ends. Rotational relaxation times from sodium titration experiments are shown in Figure 4. R is essentially constant over the entire range of added sodium ion concentration, even though P_{app}(SKRI) increases more than 3-fold over this range. Similar measurements done with the 267-bp control fragment show that P would normally be expected to increase by less than a factor 2 over this range. If the larger than expected value of τ_{SKRI} is due entirely to increased stiffness, these data suggest that the electrostatic free energy of SK 240 is minimized by a decrease in flexibility rather than by reduced static bending.

Studies of τ as a function of magnesium ion concentration are shown in Figure 5. Here, R displays a significant dependence on ionic strength, decreasing from 0.90 in 1.0 mM Tris-HCl (no added Mg^{2+}) to 0.80 when the ratio of magnesium cations to DNA phosphates is approximately 1:2. The value of R remains effectively constant with higher Mg^{2+}/phosphate ratios in spite of a 30% decrease in P_{app}(SKRI),

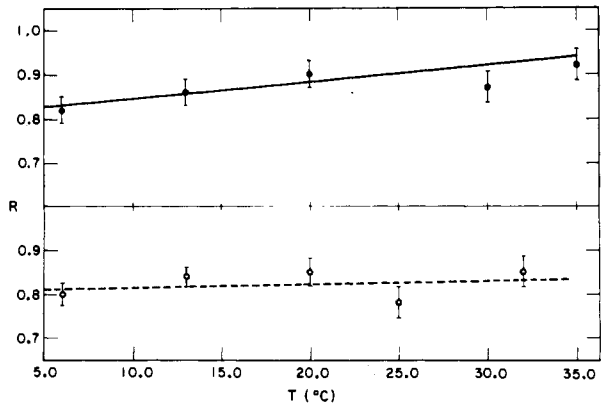

FIGURE 6: Ratios of rotational relaxation times $R = \tau_{SK}/\tau_{SKRI}$, as a function of temperature: (Upper panel) 0.03 mM NaH_2PO_4, 0.1 mM Na_2EDTA, pH 7.3; (lower panel) 1.0 mM Tris-HCl, 0.025 mM $MgCl_2$, pH 8.0. Temperature was maintained to within ±0.1 °C during the course of the experiment. The solid and dashed lines are linear least-squares fits to the data points.

supporting the view that sequence-directed bending is uncoupled from the electrostatic component of the persistence length. As is the case when Na^+ is added, P_{app}(SKRI) is significantly larger than P_{app}(267) in the presence of Mg^{2+}.

Bending in the Kinetoplast Fragments Is Weakly Temperature Dependent. Results of previous rotational relaxation studies (Hagerman, 1981) suggest that the hydrodynamic dimensions of native DNA molecules are independent of temperature below the melting temperature T_m. The values of τ corrected for viscosity and temperature (Hagerman, 1981) should therefore be independent of temperature. This was verified for the 267-bp control fragment, τ scaled for temperature and viscosity varying by less than 3% over the range 6–30 °C (data not shown). Systematic variation of corrected τ values with temperature below T_m would therefore suggest the presence of a structural transition not normally observed in DNA fragments. Such a phenomenon might be anticipated in K DNA fragments, since elevated temperature produces nearly normal gel electrophoretic mobility (Wu, 1982; Marini et al., 1984).

Data showing the temperature dependence of R in two different buffers are given in Figure 6. In the presence of 1.7 mM Na^+, the measured value of R rises with increasing temperature, from 0.82 at 6.0 °C to 0.92 at 35.0 °C. This gradual temperature dependence is distinct from the behavior expected upon strand separation; melting of the helix would give rise to a sharp change in τ.

In 0.025 mM Mg^{2+}, R appears to be more weakly temperature dependent, suggesting that Mg^{2+} may play some role in stabilizing the bent conformation, whether by stabilization of the helix junctions or by stronger screening of the electrostatic interactions. It should be noted, however, that experimental limits on the accuracy of R values makes the apparent distinction between Mg^{2+}- and Na^+-containing solutions of marginal significance.

Discussion

We have compared the relative rates of rotational diffusion of two restriction fragments, each containing a region of bent helical structure, to quantitate the amount of bending in these fragments. The ratio of rotational relaxation times is consistent with an angular displacement of the helix axis by 9° at junctions between tracts of oligo(dA)·oligo(dT) containing five or more base pairs and the flanking sequences, presumed to be B-form DNA. The calculated average bend angle between the two ends of a fragment with the bending locus located near its center is 84°, a conclusion not dependent on the assumption of a junction-bending model. This analysis is, of course, subject to several assumptions and approximations dealt with below.

The tracts of oligo(dA)·oligo(dT) are assumed to contain an altered (non-B) helical form which, in some way, is responsible for sequence-directed bending in kinetoplast DNA. In earlier studies, we established that ApA and TpT dinucleotides are repeated with high periodicity in the kinetoplast sequence (Marini et al., 1982), but it was not then possible to determine whether sequence-directed bending was governed by dinucleotides or longer sequences. The majority of A-T base pairs in the kinetoplast sequence are contained in tracts of five or six contiguous A's or T's phased at approximately 10 base pair intervals. To account successfully for sequence-directed bending with a junction model requires that the DNA helix be alternately bent in opposing directions approximately every half-helical turn. This is possible if the base pairs in A-T tracts are tilted from the perpendicular to the local helix axis and if the tilted base pairs stack parallel to the base pairs in the adjacent segments of B-DNA.

Evidence has been accumulating for some time that poly(dA)·poly(dT) is unusual in its structure and physical properties; the helical repeat of poly(dA)·poly(dT) is known to be anomalous (Peck & Wang, 1981), and the sequence apparently cannot form nucleosomes under conditions where nucleosomes can be reconstituted from other DNAs (Simpson & Kunzler, 1979). Other evidence for an anomalous structure comes from Raman scattering studies (Thomas & Peticolas, 1983), which indicate the presence of an unusual mixed C_2'-endo and C_3'-endo sugar conformation in the polymer. Fiber diffraction experiments by Arnott and co-workers (Arnott et al., 1983) are also consistent with an unusual structure for poly(dA)·poly(dT); their data led them to propose a model in which one strand [poly(dA)] is similar in structure to the A conformation of DNA and the other strand is similar to the B form. Overall, the structure contains significant base pair tilt.

In applying the junction-bending model to interpret the physical properties of kinetoplast DNA, we have been forced to make a number of assumptions because only a limited number of parameters can be evaluated from the experimental data. The principal quantities determined here, such as the overall bend angle, are not very sensitive to the details of the model, but some of the underlying assumptions may need to be reevaluated in future work: First, we assume that the bends at the 5′ and 3′ ends of an A tract are the same. This may be incorrect, since almost all of the tracts are flanked by a C at the 5′ end and a T at the 3′ end, increasing further their inherently asymmetric character. Second, we have assumed a helical repeat of 10.0 bp in the oligo(dA)·oligo(dT) tracts, consistent with observations for the polymer. Changes in this value for the helical repeat will generally lead to changes in the apparent value of θ_J; we expect that this question can be clarified in future experiments. Third, we have assumed that the DNA helix is isotropically flexible, meaning that thermal bending (as opposed to systematic bending) is equally probable in all directions. This assumption seems a good one, since in some preliminary calculations we observed that favoring roll, tilt, or some combination of the two made no quantitative difference; the dimensional statistics of the model chains depend only on the ratio h/P and not on the relative values of the constants a and b.

Finally, we have assumed that the bending stiffness is constant along the contour of the fragment, an assumption that cannot be strictly correct if the apparent increased stiffness of K DNA reflects higher rigidity for the oligo(dA)·oligo(dT)

tracts, since in that case P would be a function of position in the chain. Detailed examination of this question must await calculations in which the stiffness is sequence-dependent (S. D. Levene and D. M. Crothers, unpublished data), for which independent estimates of the necessary parameters will probably be needed. Qualitatively, however, increased stiffness in the dA·dT tracts would affect the SK fragment more than the SKRI fragment, since in the case of SK the tracts are concentrated in the center of the molecule where their reduced flexibility would have the greatest effect. The net effect of neglecting this factor will be an underestimation of the extent of systematic bending, since the amount of thermal bending in the center region would be simultaneously overestimated.

We have also presented an alternative model that accounts for the increased apparent stiffness of knetoplast DNA by removing the assumption of a uniform value for the rise per base pair in bent and "normal" unbent DNAs. In some preliminary studies of the effect of sequence-dependent values of P on τ, we observed that only part of the unexpectedly large value of P_{app}(SKRI) can be accounted for, even if the oligo(dA)·oligo(dT) tracts are made to be essentially rigid. The difference in P_{app} for SKRI from the value determined for the 267-kb electrophoretically normal control fragment is consistent with a 3% increase in the unit rise for SKRI if P = 500 Å for both fragments and if the unit rise is given its usual value of 3.40 Å in the normal control. Differences in h of this magnitude seem quite plausable; variations in axial rise of the order of 30% have been observed in fiber diffraction studies of natural and synthetic DNAs (Leslie et al., 1980), and variations in h as large as 13% have been noted within a single sequence from X-ray studies of single crystals of the B DNA dodecamer d(CGCGAATTCGCG) (Dickerson & Drew, 1981; Drew et al., 1981). We believe that the true situation may lie somewhere between the two extremes; in addition to being somewhat stiffer, sequences containing junction bends probably have a larger effective unit rise than that for B DNA. Although a larger effective unit rise may come from an increased unit rise in the oligo(dA)·oligo(dT) tracts, an important contribution to the unit rise might also be anticipated from the structural dislocations due to the helix–helix junctions. We expect to address this question in future experiments.

The issue of the relationship between DNA sequence and flexibility is an interesting one that warrants further study. To our knowledge, no one has reported significant departures of P from values considered to be normal (approximately 500 Å at 0.1 M salt) for any DNA restriction fragment. Some studies have been reported by Hogan et al. (1983) using triplet decay anisotropy to measure apparent twisting and bending force constants for a number of synthetic double-stranded polynucleotides, but aspects of anisotropy decay theory are still controversial (Allison & McCammon, 1984), and hydrodynamic theory appears to provide a more direct approach. Recent transient electric dichroism studies by Chen et al. (1985) examined the alternating copolymer poly(dA-dT) and found a persistence length about half that characteristic of natural DNA.

Hagerman (1984) has published a comparative study, similar to ours, of the rate of rotational diffusion of a symmetric 242-bp K DNA fragment containing two nearly in-phase bending loci, compared to the rate for an unrelated 242-bp fragment derived from ΦX-174 DNA. His value of 52° for the total bend angle results from use of the hydrodynamic equations for the once-bent rod and is clearly significantly smaller than our estimated of an 84° bend angle in a fragment containing only one bending locus. The difference is mainly due to Hagerman's assumption that P_{app} is the same in the two fragments, but it also reflects other simplifications, such as concentrating the bending at a single point and neglecting the contribution of residual thermal flexibility, as pointed out in the caption to Figure 3. We find that computer generation of the helix trajectory of the symmetric 242-bp fragment studied by Hagerman, using the 9° junction-bending model we derived from our results, predicts an overall bend of 112°. Possibly, this large degree of bending is responsible for the marked ionic strength dependence of bending that he reported.

One popular concept not considered in detail here is the purine clash model, as proposed by Calladine (1982) and elaborated on by Dickerson (1983). We have shown previously (Levene & Crothers, 1983) that the Calladine model as originally stated does not predict sequence-directed bending in K DNA. Hagerman (1984) introduced an ad hoc modification of the model, which removes compensatory roll at the points adjacent to the purine–pyrimidine transition; this approach seems more successful. However, it is difficult to see how the model can be made consistent with the observation that increased temperature reduces bending. Furthermore, the average amount of roll observed in the dodecamer crystal is substantially smaller than the amount needed to account for the estimated degree of bending in the kinetoplast fragment. Recent studies on the electrophoretic properties of model sequences (Koo et al., 1986) clearly support the junction-bending model.

References

Allison, S. A., & McCammon, J. A. (1984) *Biopolymers 23*, 363–375.

Arnott, S., Chandrasekaran, R., Hall, I. H., & Puigjaner, L. C. (1983) *Nucleic Acids Res. 11*, 4141–4155.

Broersma, S. (1960) *J. Chem. Phys. 32*, 1626–1631.

Calladine, C. R. (1982) *J. Mol. Biol. 161*, 343–352.

Chen, H. H., Rau, D. C., & Charney, E. (1985) *J. Biomol. Struct. Dyn. 2*, 709–717.

Dickerson, R. E. (1983) *J. Mol. Biol. 196*, 419–441.

Dickerson, R. E., & Drew, H. R. (1981) *J. Mol. Biol. 149*, 761–786.

Drew, H. R., Wing, R. M., Takano, T., Broka, C., Tanaka, S., Itakura, K., & Dickerson, R. E. (1981) *Proc. Natl. Acad. Sci. U.S.A. 78*, 2179–2183.

Hagerman, P. J. (1981) *Biopolymers 20*, 1503–1535.

Hagerman, P. J. (1983) *Biopolymers 22*, 811–814.

Hagerman, P. J. (1984) *Proc. Natl. Acad. Sci. U.S.A. 81*, 4632–4636.

Hagerman, P. J., & Zimm, B. H. (1981) *Biopolymers 20*, 1481–1502.

Hogan, M., LeGrange, J., & Austin, B. (1983) *Nature (London) 304*, 752–754.

Kidane, G. Z., Hughes, D., & Simpson, L. (1984) *Gene 27*, 265–277.

Kirkwood, J. G., & Riseman, J. (1948) *J. Chem. Phys. 16*, 565–573.

Koo, H.-S., Wu, H.-M., & Crothers, D. M. (1986) *Nature (London) 320*, 501–506.

Leslie, A. G. W., Arnott, S., Chandrasekaran, R., & Ratliff, R. L. (1980) *J. Mol. Biol. 143*, 49–72.

Levene, S. D., & Crothers, D. M. (1983) *J. Biomol. Struct. Dyn. 1*, 429–435.

Levene, S. D., & Crothers, D. M. (1986) *J. Mol. Biol.* (in press).

Maniatis, T., Frisch, E. F., & Sambrook, J. (1982) *Molecular Cloning: A Laboratory Manual*, Cold Spring Harbor Laboratory, Cold Spring Harbor, NY.

Marini, J. C., Levene, S. D., Crothers, D. M., & Englund, P. T. (1982) *Proc. Natl. Acad. Sci. U.S.A. 79*, 7664–7668.
Marini, J. C., Effron, P. N., Goodman, T. C., Singleton, C. A., Wells, R. D., Wartell, R. M., & Englund, P. T. (1984) *J. Biol. Chem. 254*, 5417–5422.
Marquardt, D. W. (1963) *J. Soc. Ind. Appl. Math. 11*, 431–441.
Peck, L. J., & Wang, J. C. (1981) *Nature (London) 292*, 375–378.
Prunell, A., Goulet, I., Jacob, Y., & Goutorbe, F. (1984) *Eur. J. Biochem. 138*, 253–257.
Selsing, E., Wells, R. D., Alden, C. J., & Arnott, S. (1979) *J. Biol. Chem. 254*, 5417–5422.
Simpson, R. T., & Kunzler, P. (1979) *Nucleic Acids Res. 6*, 1387–1415.
Sutcliffe, J. G. (1978) *Cold Spring Harbor Symp. Quant. Biol. 43*, 77–90.
Thomas, G. A., & Peticolas, W. L. (1983) *J. Am. Chem. Soc. 105*, 993–996.
Trifonov, E. N., & Sussman, J. L. (1980) *Proc. Natl. Acad. Sci. U.S.A. 77*, 3816–3820.
Wegener, W. A., Dowben, R. M., & Koester, V. J. (1979) *J. Chem. Phys. 70*, 622–632.
Wu, H.-M. (1982) Thesis, Yale University.
Wu, H.-M., & Crothers, D. M. (1984) *Nature (London) 308*, 509–513.
Yamakawa, H. (1970) *J. Chem. Phys. 53*, 436–443.
Zhurkin, V. B. (1985) *J. Biomol. Struct. Dyn. 2*, 785–804.
Zimm, B. H. (1980) *Macromolecules 13*, 592–602.

Proflavin Binding to Poly[d(A-T)] and Poly[d(A-br^{5}U)]: Triplet State and Temperature-Jump Kinetics†

Alan F. Corin‡ and Thomas M. Jovin*
Abteilung Molekulare Biologie, Max-Planck-Institut für Biophysikalische Chemie, D-3400 Göttingen, FRG
Received September 5, 1985; Revised Manuscript Received February 27, 1986

ABSTRACT: The delayed fluorescence properties of proflavin have been exploited in studies of the excited-state binding kinetics of the dye to poly[d(A-T)] and its brominated analogue poly[d(A-br^{5}U)] at room temperature and pH 7. The two analyzed luminescence decay times of the DNA–dye complex are dependent on the total nucleic acid concentration. This dependence is shown to reflect a temporal coupling of the intrinsic delayed emission decay rates with the dynamic chemical kinetic binding processes in the excited state. Temperature-jump kinetic studies conducted on the brominated polymer and corresponding information on poly[d(A-T)] from a previous study [Ramstein, J., Ehrenberg, M., & Rigler, R. (1980) *Biochemistry 19*, 3938–3948] provide complementary information about the ground state. In the ground state, the poly[d(A-T)]–proflavin complex has one chemical relaxation time, which reaches a plateau at high DNA concentrations. The brominated DNA–dye complex exhibits two relaxation times: a faster relaxation mode that behaves similarly to that for the unhalogenated DNA and a slower relaxation mode that is apparent at high DNA concentrations. The ground-state kinetic data are analyzed in terms of two alternative models incorporating series and parallel reaction schemes. The former consists of two sequential binding steps—a fast bimolecular process followed by a monomolecular step—while the latter consists of two coupled bimolecular steps. A similar analysis for the excited-state data yields reasonable kinetic constants only for the series model, which, in accordance with previous proposals for acridine intercalators, consists of a fast outside binding step followed by intercalation of the dye. A comparison of the ground- and excited-state kinetic parameters reveals that the external binding process is much stronger and the intercalation is much weaker in the excited state. That the excited-state data are only consistent with the series model suggests that delayed luminescence studies may provide a general tool for distinguishing between the two kinetic mechanisms. In particular, we demonstrate the use of delayed luminescence spectroscopy as a tool for probing dynamic DNA–ligand interactions in solution.

Acridine dyes exhibit a number of biologically interesting phenomena that have been the subject of extensive investigations. These planar heteronuclear chromophores demonstrate antibacterial (Albert, 1973) and mutagenic properties (Brenner et al., 1961; Streisinger et al., 1966) and are used as probes for visualizing chromosomes (Caspersson et al., 1969). Another useful feature of acridine–DNA interactions is the metachromasia exhibited by single- vs. double-stranded nucleic acids [Porumb, 1978; Peacocke (1973) and references cited therein].

Two modes of binding have been attributed to the acridine–DNA system at low dye concentrations (submicromolar) and DNA to dye (P/D)[1] ratios >10: (1) an external binding mode in which the electrostatic forces between the positively charged acridine (at neutral pH) and the polyanionic DNA polymer play a major role; (2) a stronger internal mode with

† A.F.C. was supported by a Max Planck Society fellowship.
‡ Present address: Life Sciences Division, Eastman Kodak Co., Rochester, NY 14650.

[1] Abbreviations: T jump, temperature jump; P/D, DNA (in nucleotide units) to dye ratio; Tris-HCl, tris(hydroxymethyl)aminomethane hydrochloride; EDTA, ethylenediaminetetraacetic acid.

0006-2960/86/0425-3995$01.50/0